Neuron, Volume 63

Supplemental Data

The microRNA *bantam* Functions in Epithelial Cells to Regulate Scaling Growth of Dendrite Arbors in *Drosophila* Sensory Neurons

Jay Z. Parrish, Peizhang Xu, Charles C. Kim, Lily Yeh Jan, and Yuh Nung Jan

Table S1. Alleles used in this study.

Mutant alleles	Gene name	Source
$ban^{\Delta 1}$	bantam	Cohen Lab (Brennecke et al., 2003)
shr^{1}	shrunken	Bloomington Stock Center (BL396)
std^{1}	staroid	Bloomington Stock Center (BL411)
twf^{EP3701}	twinfillin	Bloomington Stock Center (BL17157)
Ddc^{k02104}	Dopa decarboxylase	Bloomington Stock Center (BL10508)
Tor^{k17004}	Target of rapamycin	Bloomington Stock Center (BL11218)
$Tor^{\Delta P}$	Target of rapamycin	Bloomington Stock Center (BL7014)
shf^{2}	shifted	Bloomington Stock Center (BL112)
gt^{E6}	giant	Bloomington Stock Center (BL1530)
gt^{1}	giant	Bloomington Stock Center (BL53)
$Pdp1^{P205}$	Pyruvate dehydrogenase phosphatase	Bloomington Stock Center (BL6932)
$Tctp^{EY09182}$	Translationally controlled tumor protein	Bloomington Stock Center (BL16927)
$InR93^{Dj\text{-}4}$	Insulin Receptor	Bloomington Stock Center (BL9554)
InR^{E19}	Insulin Receptor	Bloomington Stock Center (BL9646)
Akt^{104226}	Akt/Protein Kinase B	Bloomington Stock Center (BL11627)
Akt^{9}	Akt/Protein Kinase B	Tian Xu
$step^{k08110}$	steppke	Bloomington Stock Center (BL10770)
$cdc2^{c2}$	cdc2	Bloomington Stock Center (BL6632)
$Cdk4^{3}$	Cyclin-dependent kinase 4	Bloomington Stock Center (BL6644)
$Rheb^{AV4}$	Rheb	Bloomington Stock Center (BL9690)
$slik^{KG04837}$	Sterile20-like kinase	Bloomington Stock Center (BL14435)
klu^{09036}	klumpfuss	Bloomington Stock Center (BL11733)
$chico^{1}$	chico	Bloomington Stock Center (BL10738)
$CG3511^{1}$	CG3511	Bloomington Stock Center (BL8198)
$Stat92E^{06346}$	Signal-transducer and activator of transcription protein at 92E	Bloomington Stock Center (BL11681)
tkd^{1}	thickoid	Bloomington Stock Center (BL426)
Csk^{j1D8}	C-terminal Src kinase	Bloomington Stock Center (BL10244)
$l(2)gl^{1}$	lethal giant larvae	Jan lab
$l(2)gl^{4}$	lethal giant larvae	Bloomington Stock Center (BL9042)
$G\text{-}s\alpha 60AB^{19}$	G protein sα 60A	Bloomington Stock Center (BL6339)
$Eip75B^{a81}$	Ecdysone-induced protein at 75B	Bloomington Stock Center (BL23654)
br^{1}	broad	Bloomington Stock Center (BL3994)
esc^{21}	extra sex combs	Bloomington Stock Center (BL3623)
fry^{1}	furry	Jan lab
sav^{3}	salvador	Jan lab
b-6-22	unknown	Jan lab (SY, unpublished data)

Deficiencies	**Source/Description**
Df(3L)Exel6086	Bloomington Stock Center (BL7565)
Df(3L)ED4177	Bloomington Stock Center (BL8048)

UAS Transgenes	**Source**
UAS-ban-A	Cohen Lab (Brennecke et al., 2003)
UAS-ban-B	Cohen Lab (Brennecke et al., 2003)
UAS-ban-C	Cohen Lab (Brennecke et al., 2003)
UAS-ban-D	Cohen Lab (Brennecke et al., 2003)
UAS-ban-PX	This study
UAS-Akt	Bloomington Stock Center (BL8191)
UAS-Pten	Tian Xu
UAS-Pi3K (CAAX)	Bloomington Stock Center (BL8294)
UAS-*Dcr-2*	Bloomington Stock Center (BL24650)
UAS-*Akt*(RNAi)	Vienna Drosophila Resource Center (v2902)

Gal4 Drivers	**Source**
Actin-Gal4	Jan lab
HS-Gal	Bloomington Stock Center (BL2077)
Twist-Gal4	Bloomington Stock Center
Mhc-Gal4	Bloomington Stock Center
arm-Gal4	Bloomington Stock Center (BL1560)
69B-Gal4	Bloomington Stock Center (BL1774)
ppk-Gal4	Jan lab
Lsp2-Gal4	Bloomington Stock Center (BL6357)
Mai311-Gal4	Quan Yuan
P0206-Gal4	Pierre Leopold
477-Gal4	Jan Lab (Grueber et al., 2003a)
221-Gal4	Jan Lab (Grueber et al., 2003a)
ss-Gal4	Michael Kim, unpublished
elav-Gal4	Bloomington Stock Center (BL458)

Reporters	**Source**
tgph	Bloomington Stock Center (BL8165)
arm^{weep}	Fabrice Roegiers (Clyne et al., 2003)
MHC^{weep}	Fabrice Roegiers (Clyne et al., 2003)
$Nrx\text{-}IV^{CA06597}$	Flytrap (flytrap.med.yale.edu)
UAS-mCD8-RFP	Elizabeth Gavis
UAS-mCD8-GFP	Bloomington Stock Center (many stocks)
UAS-mCD2-Cherry	Jan lab (Sabina Zimmerman, unpublished)
ppk-EGFP	Jan lab, (Grueber et al., 2003b)
tub-EGFP	Cohen Lab (Brennecke et al., 2003)
tub-EGFP.ban	Cohen Lab (Brennecke et al., 2003)

Figure Legends

Figure S1. Measurement of dendrite coverage index.

The dendrite coverage index was defined as the ratio of the territory covered by the dorsal field of a dorsal cluster PNS neuron to the total dorsal area of that hemisegment. The ventral-most boundary for the dorsal field was generated by drawing a straight line connecting a neuron of interest to the corresponding neuron in the adjacent anterior and posterior segments.

Figure S2. Dendrites in multiple classes of da neurons exhibit a rapid growth phase followed by a scaling growth phase.

(A) Representative images of class I da neurons (Grueber et al., 2002) visualized with *Gal4^{221}, UAS-mCD8-GFP*. Class I dendrites cover their characteristic region of the body wall by approximately 24 hr AEL and then maintain this coverage for the remainder of larval development.

(B) Representative images of class III da neurons (Grueber et al., 2002) visualized with *spineless-Gal4, UAS-mCD8-GFP*. Class III dendrites (ddaF) cover their characteristic region of the body wall by approximately 48 hr AEL and then maintain this coverage for the remainder of larval development.

Figure S3. Loss of *bantam* function causes defects in dendrite scaling.

Dendrite scaling was assessed in larvae of the indicated genotypes, represented schematically in (A), by measuring dendrite coverage index of ddaC class IV neurons (B) and the number of times dendrites of a single ddaC class IV neuron cross the dorsal midline (C). For this and all subsequent figures, error bars represent SEM, * denotes $p < 0.05$ and ** denotes $p < 0.001$. $n > 5$ for each genotype.

Figure S4. *bantam* regulates dendrite scaling of a subset of da neurons.
Dendrite growth of class III (A) or class I (B) da neurons in *bantam* mutant larvae was visualized using *spineless-Gal4* or $Gal4^{221}$, respectively, to drive expression of mCD8-GFP in the indicated neurons. Dendrite growth was monitored using live confocal microspcopy and representative images from 96hr AEL wild type (wt) or *bantam* mutant ($ban^{\Delta 1}$) are shown.

Figure S5. *bantam* affects dendrite dynamics. Time-lapse imaging of class IV ddaC neurons from control (A) or $bantam^{\Delta 1}$ (B) larva. Dynamic behavior of terminal dendrites was monitored for the dorsal portion of the ddaC dendritic arbor, which extends from the soma to the dorsal midline in one dimension (along the dorsal/ventral axis) and is delimited by segment boundaries in the other dimension (anterioposterior axis), corresponding roughly to a 250 x 250 μm region in 96 hr AEL larvae. Dynamic terminals were classified as follows: growing terminals (increased in length over the time-lapse); newly formed terminals (dendrite branch initiation events that occur over the time-lapse; a subset of the “growth” category); retracting terminals (reduced length over the time-lapse); and lost branches (terminal dendrites that completely retract and are lost over the time-lapse; a subset of the “retraction” category). For comparable portions of the arbors in (A) and (B), terminal dendrite loss and branch initiation are represented by red and blue circles, respectively, and dynamics are depicted in traces with dendrite retraction and growth depicted by red and blue lines, respectively. Neurons were imaged at 24 hr intervals beginning at 72 hr AEL using live confocal microscopy. Prior to imaging and between imaging sessions larvae were grown on yeasted grape juice agar plates at 25°C. Representative control and *bantam* mutant neurons are shown at 72 hr and 96 hr AEL. Scale bars are 50 μm.

Figure S6. *bantam* regulates dendrite scaling independent of pathways known to regulate dendritic tiling.

(A-D) *bantam* regulates dendrite scaling independent of pathways known to regulate dendritic tiling. Dendrite coverage at 96 hr AEL in *esc* (A), *esc; ban* (B), *fry* (C) or *ban, fry* (D) mutant larvae was visualized using *ppk*-EGFP. The interface of two ddaC neurons at the dorsal midline (blue hatched box) is shown below each image. (E) Quantitation of dendrite coverage index. *n* > 10 for each genotype. Scale bars are 50 μm.

Figure S7. *bantam* cell-autonomously promotes dendrite growth

MARCM analysis was conducted as previously described (Grueber et al., 2002). MARCM clones were imaged from fixed samples and for each clone the entire dendrite arbor was captured and traces were generated using Neurolucida software. From these traces we calculated the total number of dendrite branchpoints for ddaE class I (A) or dda C class IV (B) dendrites as well as the total dendrite length of ddaE class I (A) or dda C class IV (B) dendrites in control or *bantam*$^{\Delta 1}$ mutant MARCM clones. *n* > 6 neurons for each genotype.

Figure S8. *bantam* function in epithelial cells is sufficient for dendrite scaling. The ability of transgenic expression of *bantam* directed by a variety of Gal4 drivers to rescue dendrite growth and larval growth defects of *bantam* mutants was assayed at 96 hr AEL. Representative images for rescue data from 96 hr AEL larvae presented in Figure 6A-6C are shown. Genotypes are as follows: (A) *UAS-ban/+; ppk-EGFP* (B) *UAS-ban/+; ban*$^{\Delta 1}$*, ppk-EGFP* (C) *elav-Gal4/+*; *UAS-ban/+; ban*$^{\Delta 1}$*, ppk-EGFP* (D) *UAS-ban/Mhc-Gal4; ban*$^{\Delta 1}$*, ppk-EGFP* (E) *UAS-ban/twi-Gal4; ban*$^{\Delta 1}$*, ppk-EGFP* (F) *UAS-ban/69B-Gal4; ban*$^{\Delta 1}$*, ppk-EGFP* (G) *UAS-ban/HS-Gal4; ban*$^{\Delta 1}$*, ppk-EGFP*.

References

Brennecke, J., Hipfner, D.R., Stark, A., Russell, R.B., and Cohen, S.M. (2003). bantam encodes a developmentally regulated microRNA that controls cell proliferation and regulates the proapoptotic gene hid in Drosophila. Cell *113*, 25-36.

Clyne, P.J., Brotman, J.S., Sweeney, S.T., and Davis, G. (2003). Green fluorescent protein tagging Drosophila proteins at their native genomic loci with small P elements. Genetics *165*, 1433-1441.

Grueber, W.B., Jan, L.Y., and Jan, Y.N. (2002). Tiling of the Drosophila epidermis by multidendritic sensory neurons. Development *129*, 2867-2878.

Grueber, W.B., Jan, L.Y., and Jan, Y.N. (2003a). Different levels of the homeodomain protein cut regulate distinct dendrite branching patterns of Drosophila multidendritic neurons. Cell *112*, 805-818.

Grueber, W.B., Ye, B., Moore, A.W., Jan, L.Y., and Jan, Y.N. (2003b). Dendrites of distinct classes of Drosophila sensory neurons show different capacities for homotypic repulsion. Curr Biol *13*, 618-626.

Supplemental Figure 1

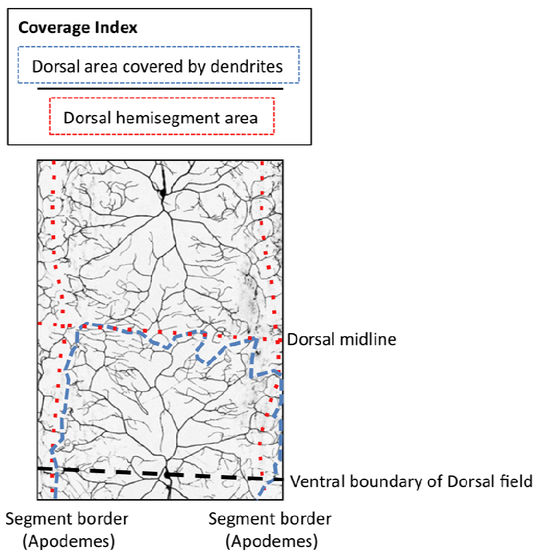

Coverage Index = 0.94

Supplemental Figure 2

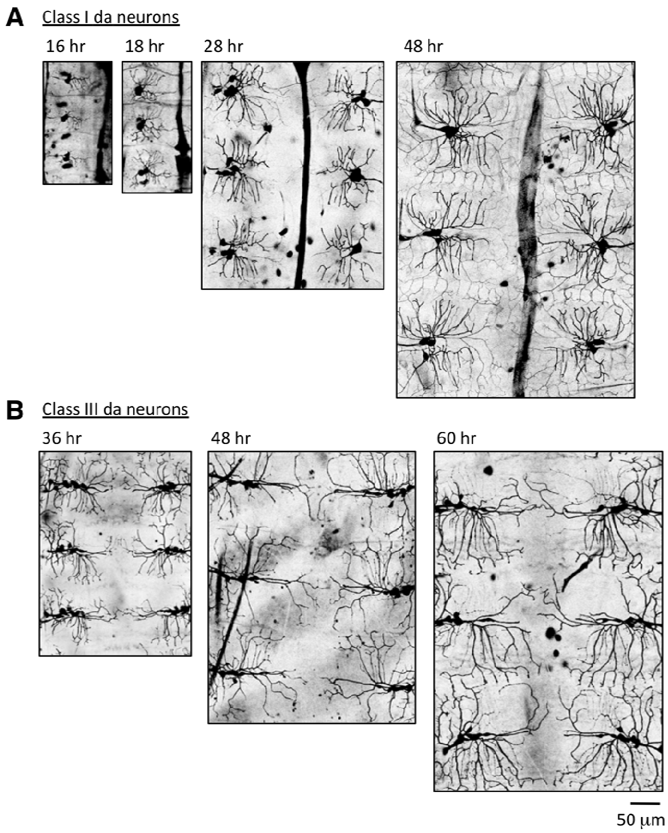

Supplemental Figure 3

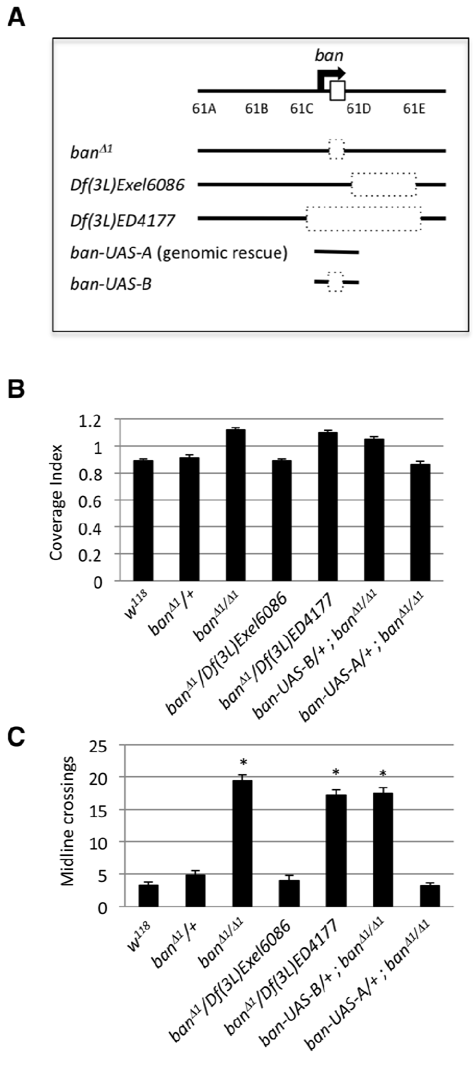

Supplemental Figure 4

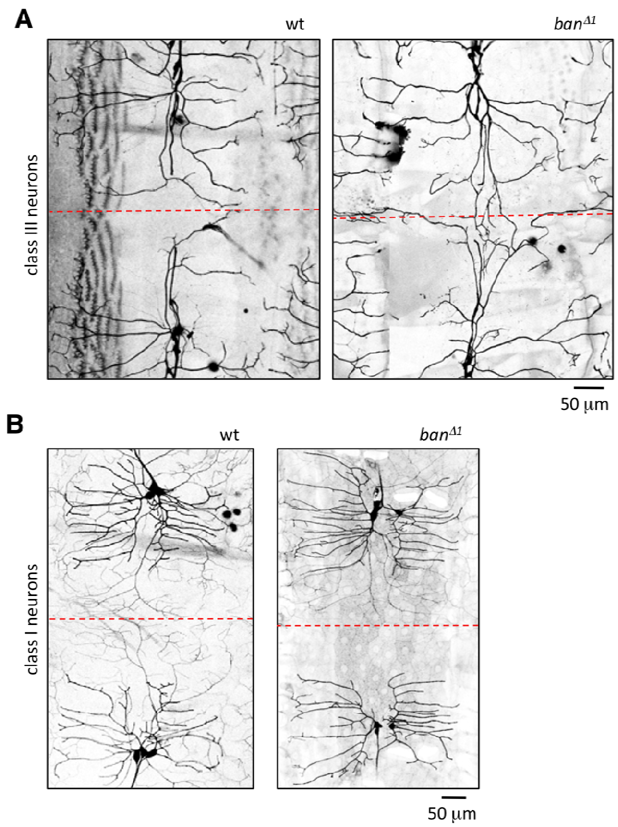

Supplemental Figure 5

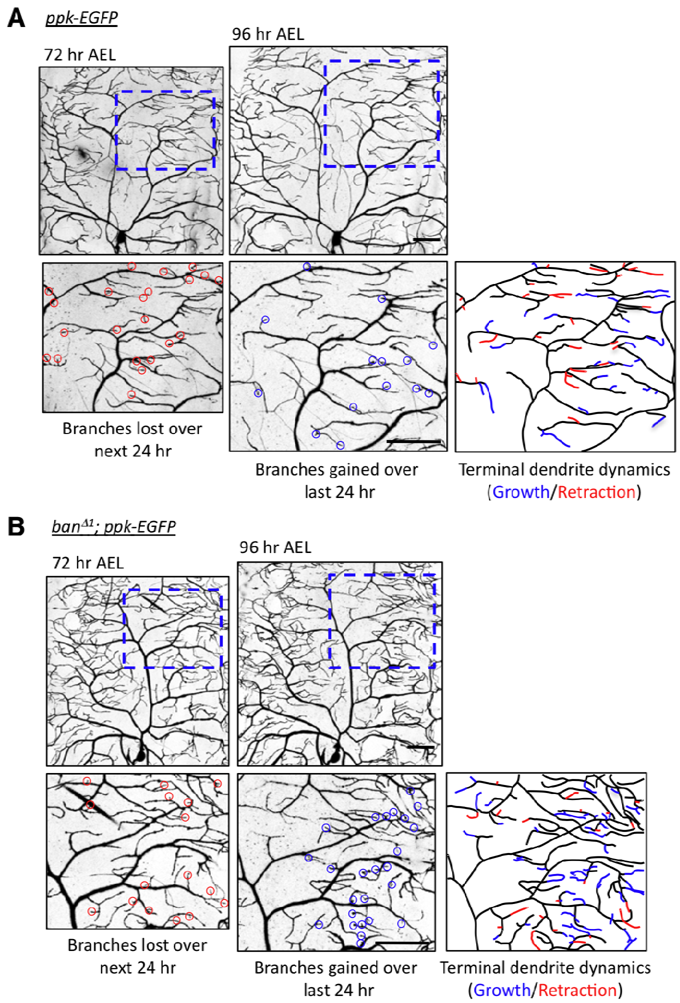

Supplemental Figure 6

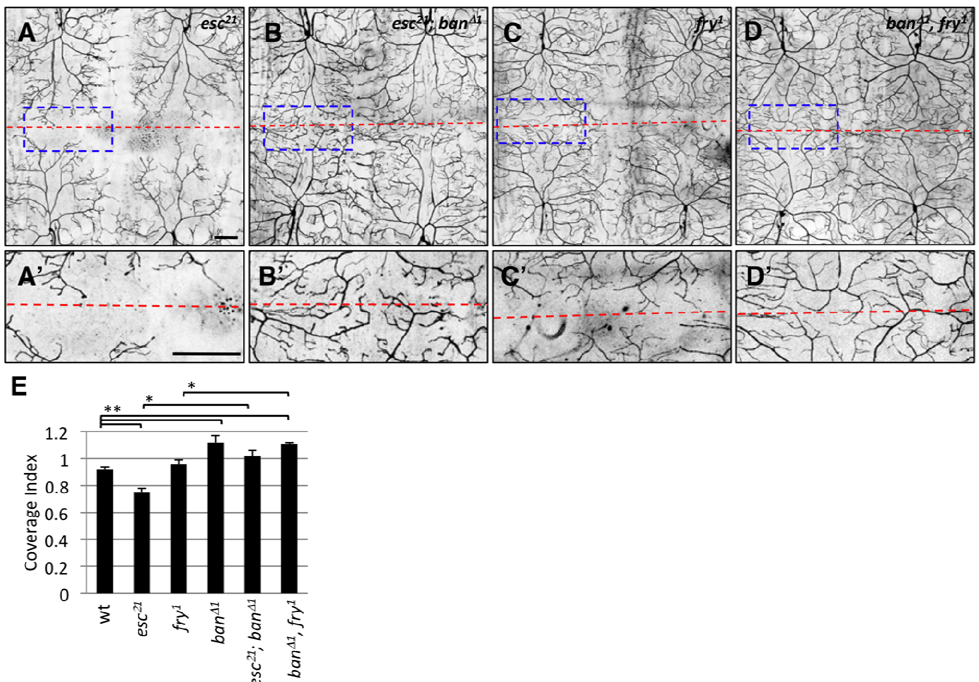

Supplemental Figure 7

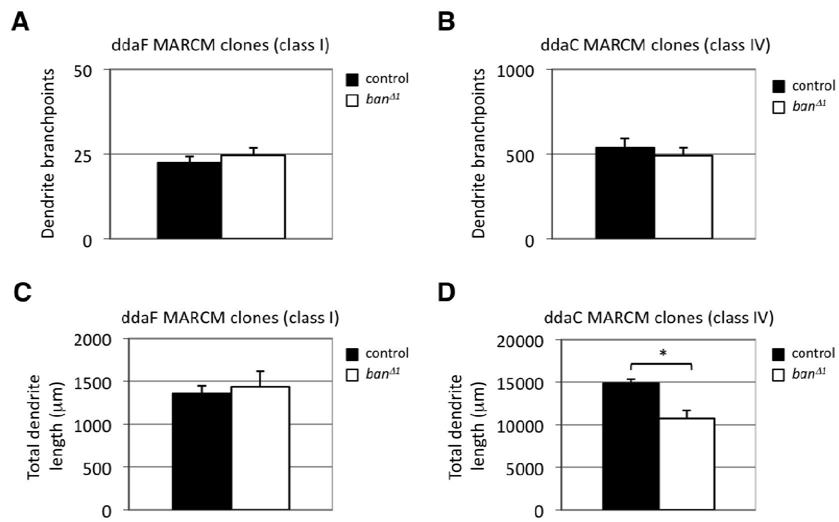

Supplemental Figure 8